Journal of Thermal Analysis and Calorimetry, Vol. 59 (2000) 171–186

Dedicated to Prof. Edith A. Turi in recognition of her leadership in education

QUARTZ MICROBALANCE MICROCALORIMETRY
A new method for studying polymer-solvent thermodynamics

A. L. Smith and H. M. Shirazi

Chemistry Department, Drexel University, Philadelphia, PA 19104, USA

Abstract

We have developed a sensitive method of determining enthalpy changes for gas-surface interactions: quartz microbalance microcalorimetry. We mount in an isoperibol environment both sample and reference combinations of a quartz crystal microbalance (QCM) in intimate thermal contact with a heat flow sensor. We coat the sample QCM with a thin (~1 μm) polymer film. By exposing the film to ethanol vapor, we measure simultaneously the change in mass per unit area (to ±0.25 ng cm^{-2}) and the resulting heat flows (to ±50 nW) when the polymer adsorbs or desorbs ethanol. The molar enthalpies of sorption of ethanol vapor in Tecoflex, an aliphatic polyurethane elastomer, are $\Delta_{adsorption}H$= –53±8 kJ mol^{-1} and $\Delta_{desorption}H$= 52±3 kJ mol^{-1}.

Keywords: heat conduction calorimetry, quartz crystal microbalance, thin-film calorimetry, sorption enthalpies of polymers

Introduction

Understanding the thermodynamics of polymer-solvent systems gives polymer scientists a basis from which to explain and relate many important physical and chemical properties of polymers. Examples are the Flory-Huggins theory of polymer-solvent interactions and the resulting polymer-solvent interaction parameters [1], polymer solubility and solubility parameters [2], and heat, entropy, and volume changes for polymer-liquid mixtures [3]. The standard methods of thermal analysis and calorimetry have been central in studying polymer-solvent systems. Most thermodynamic studies of these systems are made with the solvent in liquid form, but these measurements are often on dilute solutions because equilibrium takes longer to establish in concentrated solutions. Inverse gas chromatography, in which the stationary phase of a GC column is the solid polymer of interest and volatile solvent probes are passed through the column, has been used to determine polymer properties such as transition temperatures, polymer-polymer interaction parameters, acid-base characteristics, solubility parameters, and crystallinity, as well as properties of the solvent vapor-solid polymer system such as enthalpies of adsorption [4].

Here we describe a new calorimetric method of investigating polymer-solvent systems: quartz microbalance/microcalorimetry [5]. We mount in an isoperibol environment both sample and reference combinations of a quartz crystal microbalance (QCM) in inti-

1418–2874/2000/ $ 5.00

Akadémiai Kiadó, Budapest
Kluwer Academic Publishers, Dordrecht

mate thermal contact with a heat flow sensor. We coat the sample QCM with a thin (~1 μm) film of a polymer above its glass transition temperature. By providing both QCM surfaces with the same slow flow of nitrogen carrier gas with different known concentrations of organic solvent vapor, we have been able to measure simultaneously the change in mass per unit area (to ±0.25 ng cm^{-2}) and the resulting heat flows (to ±50 nW) when the polymer on the sample QCM surface takes up or releases solvent vapor. Such data have been analyzed to give the molar enthalpy of sorption of ethanol vapor in an aliphatic polyurethane.

The apparatus and its calibration

The quartz crystal microbalance

Although the piezoelectric effect has been known since the 19th century, the commercial development of quartz crystal devices which oscillate at precisely defined resonant frequencies and which can be incorporated as passive elements into electronic instruments received a massive push during World War II. Today there is widespread use of quartz crystal oscillators in electronics wherever precise control of frequency is needed. Ward and Buttry [6] describe the *converse piezoelectric effect* in quartz, the process by which an applied voltage generates a mechanical deformation. They review its use in in-situ interfacial mass detection, such as in thickness monitors for thin-film preparation and chemical sensors for trace gases. Grate, Martin, and White [7] compare the acoustical and electrical properties of five acoustic wave devices used as microsensors and transducers.

The resonant frequency of a circular quartz plate oscillating in the thickness shear mode is inversely proportional to the thickness of the plate. If this thickness is increased by the deposition of material on the surface of the oscillator, its frequency will decrease. In 1959, Sauerbrey [8] derived the fractional decrease in frequency $\Delta f/f_0$ of the oscillator upon deposition of a mass Δm of material on its surface:

$$\frac{\Delta f}{f_0}=\frac{-\Delta e}{e_0}=\frac{-2f_0\Delta m}{A\sqrt{p\mu}} \tag{1}$$

Here Δe is the change in the original thickness e_0, A is the piezoelectrically active area, and ρ and μ are the density and shear modulus of quartz. By measuring the decrease in frequency one thus can determine the mass of material deposited on the crystal, and this is the principle of the quartz crystal microbalance (QCM). The application of the QCM in chemistry for sensitive detection of gases adsorbed on solid absorbing surfaces has been reviewed by Alder and McCallum [9] and again by McCallum [10].

The heat flow sensor

In heat flow calorimetry, the heat flow from sample to a heat sink is measured as a function of time, and the total heat associated with the chemical process is determined

by integration over time. Wadsö [11] has reviewed trends in isothermal heat conduction calorimetry.

The sensor in a heat conduction calorimeter is a Peltier effect thermoelectric module, or thermopile. The thermal power P detected by a thermopile is given by the Tian equation [11],

$$P=\frac{1}{S}\left[U+\tau\left(\frac{dU}{dt}\right)\right] \tag{2}$$

where P is the thermal power, S is the thermopile sensitivity, U is the thermopile voltage, and (τ is the time constant of the calorimeter). At steady state, $U=S\cdot P$, and the output voltage is proportional to the thermal power dissipated on its surface. The time constant τ of a heat conduction calorimeter is C/G, where C is the reaction vessel heat capacity and G is the thermal conductance of the thermopile. For our apparatus, τ=53 s.

The apparatus

Figure 1 shows a sketch of sample and reference mass/heat flow sensors with their associated mounts and gas sample chambers. This apparatus was constructed in Lund University while ALS was visiting on sabbatical leave in 1997. We refer to one such mass/heat flow sensor as a QCM/HCC (quartz crystal microbalance/heat conduction calorimeter) [5]. Figure 2 shows a block diagram of the whole apparatus, constructed at Drexel University. The mass sensors are 5 MHz AT-cut QCM's (Maxtek, P/N 149211-1, model SC-501-1) with dimensions: 2.45 cm in diameter and 0.33 mm in thickness. The 160 nm thick top and bottom gold electrodes on the QCM are vacuum-deposited onto a 15 nm chromium adhesion layer. The larger top electrode (12.9 mm in diameter) is used as the active surface. However, the region of the quartz exposed to the *rf* electric field is limited to that directly beneath the smaller electrode (6.6 mm in diameter) resulting in a mass sensitive area of approximately 0.32 cm^2 [12]. Both sample and reference quartz resonators are driven by *rf* oscillator circuits

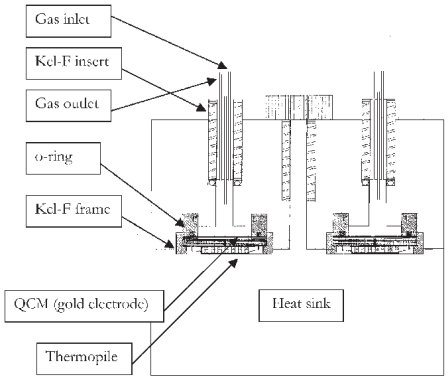

Fig. 1 Sketch of the QCM/HCC

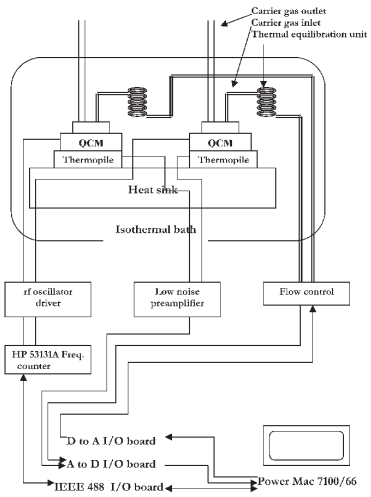

Fig. 2 Block diagram of the complete QCM/HCC apparatus

as described by Auge *et al.* [13]. The oscillation frequencies of the QCM's are measured individually with an HP 53131A frequency counter interfaced to Macintosh computer through a GPIB interface.

Each QCM rests on two *d*-shaped brass electrodes, which serve both to apply *rf* power to the QCM and to conduct heat generated on the QCM surface to the top of the thermopile. The heat flow sensors are small FC 0.45-66-05 thermopiles (Melcor, Trenton NJ). A thermopile or a thermocouple plate (TCP) consists of a large number of interconnected *n*- and *p*-doped BiTe cubes sandwiched between two ceramic plates. Four thermocouple plates are used in the QCM/HCC. Two are connected in series to form one heat flow sensor on the reference side, and the same arrangement is used for the sample side. The differential signal of the sample and reference sides is conditioned by a house-built low noise preamplifier and recorded on the same

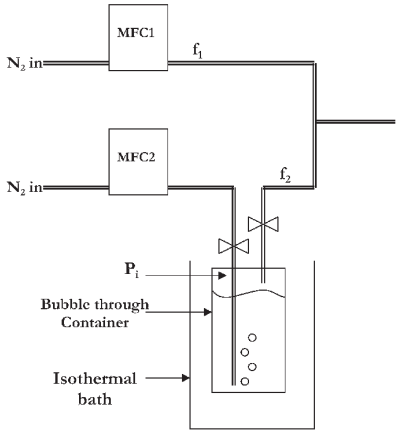

Fig. 3 The flow subsystem for vapor introduction

Macintosh computer with an A/D board under the control of Labview software (National Instruments, Inc.).

Kel-F inserts which screw into the top of both aluminum sample and reference chambers contain Teflon tubes through which gaseous samples are flowed at 1.0 atm pressure. Tsionsky and Gileadi [14] have shown that the QCM may be used to study gas phase adsorption onto a bare gold surface by employing the *supporting gas method*, in which the substance being studied is mixed with a large excess of inert gas and flowed slowly at constant P and T across the adsorbing surface. As can be seen in Fig. 3 the vapor introduction system consisted of two 0–50 scc min^{-1} mass flow controllers, MFC1 and MFC2 (Unit Technologies UFC-8100) and a bubble-through container. The nitrogen gas stream through MFC2 was directed through the bubble-through container where it was saturated with the organic solvent at a constant temperature, usually about 20°C. The resulting gas stream was then combined with that of MFC1. The entire QCM/HCC is placed in a cylindrical brass enclosure and immersed in a constant temperature bath set at 25.00°C and regulated to ±0.0001°C (Tronac 1250). Either a pure nitrogen gas stream or the gas mixture from MFC1 and MFC2 can be directed through sample and reference QCM/HCC. Both streams are temperature-conditioned by thermal equilibrium units immersed in the bath (Fig. 2). Since the gas stream flows from sample and reference chambers into the ambient atmosphere through a short tube and the flow rates are small, the sample and reference chamber pressures can be taken to be 1.0 atm.

Calibration of the two sensors

Although the accuracy of the mass measurement of the QCM can be evaluated by electrochemical methods, it is not necessary to calibrate each QCM individually when used as a balance. The Sauerbrey equation (Eq. 1) relates a change in oscillation frequency of the QCM to a change in deposited mass per unit area. The Sauerbrey

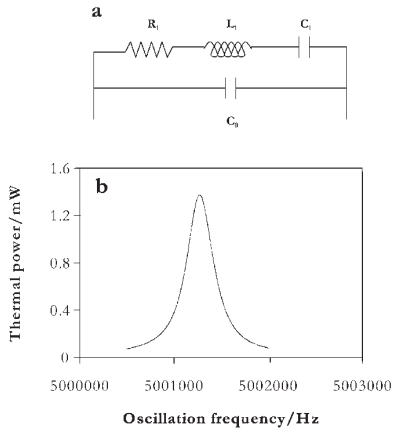

Fig. 4 Equivalent circuit of the QCM (a); Thermal power dissipated in the QCM at different frequencies (b)

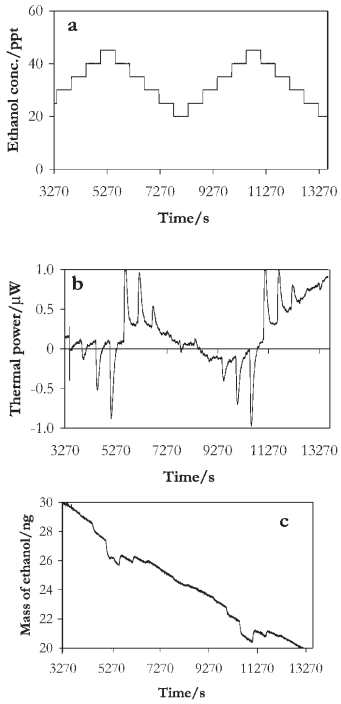

Fig. 5 Ethanol vapor concentration over two bare gold QCM surfaces (a); Difference in thermal power dissipated on two gold surfaces. For the left side of the QCM/HCC exothermic peaks are those going in the negative direction and endothermic peaks in the positive direction (b); Difference in mass signal between two QCMs (c)

equation is based on the assumption that the additional mass is coupled stiffly to the quartz resonator (see below).

In heat conduction calorimeters the calibration of heat flow sensors is usually accomplished by placing a resistor in the thermal path of the thermopile. For example, in a heat conduction solution calorimeter the resistor would be immersed in the liquid inside the calorimeter vessel. In the microbalance/calorimeter, the thermal power dissipated in the QCM itself can be used to calibrate the thermopile. The electrical equivalent circuit in Fig. 4a represents the vibrating mass of the QCM [15]. L_1 is the inertial component associated with the mass displacement. The electrical charge stored in C_1 represents the energy stored in the quartz plate. R_1 represents loss of energy as the result of internal friction or viscous damping, clamping of the QCM, and acoustic losses to the surrounding. Finally, C_0 is the static capacitance of the quartz plate with the gold electrodes, including the capacitance of the connecting cables and the physical support for the QCM. Typical values of R_1, L_1, C_0, and C_1 are given in Table 1.

Table 1 Typical values for a 5 MHz AT cut QCM

R1	14.80 Ω
L1	0.011 mH
C1	90 nF
C0	0.053 nF

For the above circuit the instantaneous power $P(t)$ dissipated in the QCM is the vector product of the current $I(t)$ and voltage $V(t)$,

$$P(t) = [I\cos(\omega t)][V\cos(\omega t+\theta)] \quad (3)$$

where θ is the phase angle between current and voltage. The *rms* power averaged over a cycle is

$$P_{rms} = I_{rms}V_{rms}\cos(\theta). \quad (4)$$

At the series resonant frequency of the RLC circuit, the inductive and capacitative contributions to the impedance cancel, θ=0, and the dissipated thermal power is due entirely to the resistance of the QCM. To calibrate the thermopiles an HP 4192A impedance analyzer was used to measure I_{rms}, V_{rms} and the phase angle θ as a function of frequency for the QCM's mounted on the thermopiles. Simultaneously, the thermal power dissipated in a given QCM was detected by its corresponding thermopile. Figure 4b shows the dissipated thermal power as a function of the impedance analyzer frequency for one of the QCM's. The high quality factor Q of the quartz resonator (ratio of frequency to full-width at half maximum of the power) is obvious. By tuning the frequency to exactly its resonant value for each QCM and measuring I_{rms}, V_{rms}, and the steady-state heat flow or thermal power (Eq. [2]), the thermal sensitivities of the right and left thermopiles were determined to be –0.343 VW^{-1} and +0.345 VW^{-1} respectively.

Experimental study of a thin polymer film

Materials

The nitrogen carrier gas was research grade 5.0 (BOC Gases). Ethanol was dehydrated 200 proof (Pharmco). The thin polymer film was comprised of Tecoflex™ SG-60D (Thermedics, Woburn MA), an aliphatic polyetherurethane elastomer whose repeat unit is shown below:

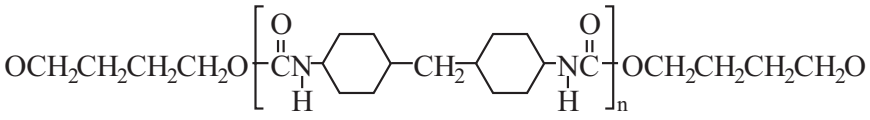

Even though its principle use is in flexible tubing for biomedical purposes we chose to study Tecoflex because it has been shown to be an effective coating for organic vapor sensors [16]. The glass transition temperature of this polymer is –20 to –40°C. The Tecoflex thin film was drop coated on a 0.159 cm^2 area on the center of the QCM's gold electrode using a 10 mg ml^{-1} chloroform solution. The shift in the oscillation frequency of the QCM corresponded to a deposited mass per unit area of 75.5 μg cm^{-2} and a total polymer mass of 12.7 μg. Based on the mass and density of the Tecoflex, the mean thickness of the film was 0.7 μm. Visual inspection of the drop-coated film under a microscope revealed no gross non-uniformities, but we did not measure the film thickness.

Results

Labview acquisition and control software for this apparatus can be programmed to control MFC1 and MFC2 to provide a stepwise increase or decrease of volatile organic vapor concentration over a defined time interval. One such flow pattern for ethanol vapor is shown in Fig. 5a, where vapor concentration in parts per thousand is computed from the relative flow rates and the vapor pressure of ethanol in the bubble-through container. Ethanol vapor concentration remains fixed for 470 seconds and then is increased or decreased by 5 ppt.

In order to determine the sensitivity of the differential mass and heat flow sensors, to assess long-term drift, and to find out how well matched sample and reference QCM/HCC's were, we placed a bare quartz crystal resonator in both sample and reference sides and subjected them both simultaneously to the flow pattern for ethanol vapor shown in Fig. 5a. The QCM's were each cleaned in Piranha solution (one part 30% H_2O_2 in three parts 98% H_2SO_4) before use. Figure 5b shows the time-synchronized differential thermal power signal from the heat flow sensors in microwatts. For ethanol concentrations of 20–25 ppt (7270–8770 s), the drift in baseline was about 0.3 μW and the standard deviation of the signal from this trendline was 50 nW. We take this as the sensitivity of the heat flow measurements. These data were taken on a sensitive preamplifier gain setting, 0.3 μV full range.

For the QCM/HCC on the left side of the apparatus (the reference side), negative-going peaks in the thermal power signal correspond to exothermic events, positive-going to endothermic events. For the right (sample) side, positive-going peaks are exothermic. We have shown [5] that for a simple adsorption or desorption of gas from the film on the QCM the thermal signal should be proportional to the time derivative of the mass signal. In effect, when the mass of adsorbed gas abruptly increases, the flow of heat from the film to the heat sink is a pulse whose width is determined by the time constant of the heat flow calorimeter and whose integrated area is proportional to the evolved heat of adsorption. Thus, the exothermic peaks observed when the ethanol vapor concentration increases from 30 to 35 to 40 ppt must be due to some excess adsorption of ethanol in the sample QCM/HCC compared to the reference QCM/HCC. We are not sure why this occurs, but think that it may be due to slightly

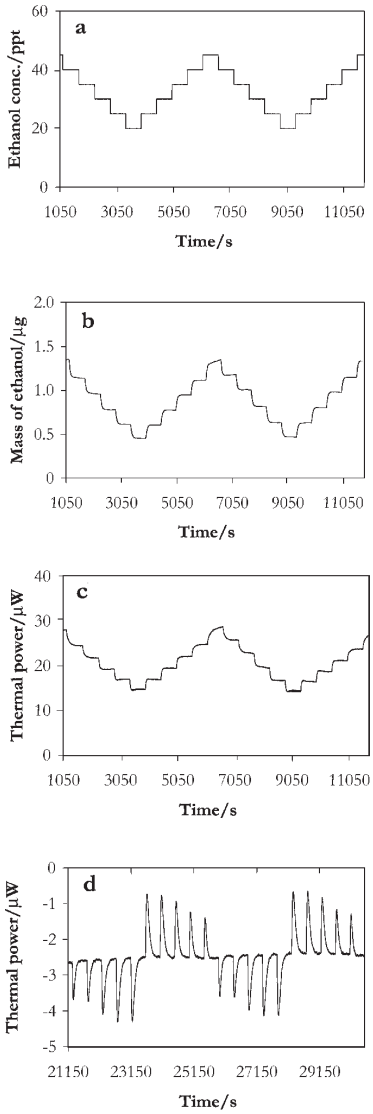

Fig. 6 Ethanol vapor concentration above the Tecoflex film (a); Mass of ethanol sorbed into the Tecoflex film (b); Thermal power for ethanol sorption in Tecoflex with both QCMs on. The Tecoflex film is placed in the right side of the QCM/HCC. For the right side the positive-going peaks are exothermic and the negative-going peaks are endothermic (c); Thermal power for ethanol sorption in Tecoflex with the right QCM off. The Tecoflex film is place in the right side of the QCM/HCC. For the right side the positive-going peaks are exothermic and the negative-going peaks are endothermic (d)

differing adsorption of ethanol by the Teflon-coated o-rings holding the quartz crystal from above. The peaks may also be due to ethanol adsorption on the bare gold electrode or the surrounding quartz of the QCM surface, as discussed by Tsionsky and Gileadi [14]. The observed width of these thermal peaks is due largely to the 53 second time constant of the heat flow calorimeters, but slow adsorption/diffusion processes may also contribute. Corresponding endothermic peaks are observed when the ethanol vapor concentration is decreased stepwise from 40 to 35 to 30 ppt and ethanol is desorbed from the QCM surface.

The corresponding difference in mass signals from the two QCM's is shown in Fig. 5c. Over the entire run the drift in baseline is about 1 pg s^{-1}. The regions of departure of the signal from this trendline, observed around 5270 s and 10900 s, occur during the times at which the ethanol vapor concentrations are largest. These mass change signals are much smaller than those observed when the QCM is coated with polymer, and are probably due to slightly differing physical adsorption of ethanol on the two bare QCM surfaces. In a time region which exhibits no such signals, the standard deviation of the mass signal from its trendline is .0137 Hz, or 0.25 mg cm^{-2}, a figure which we take as the mass-per-unit-area sensitivity of the QCM/HCC.

The bare gold QCM in the sample side was then replaced with the QCM coated with Tecoflex SG-60 (film thickness 0.7 μm, mass 12.7 μg, area 0.159 cm^2) and a similar flow pattern of stepwise changes in ethanol vapor concentration (Fig. 6a) across both sample and reference QCM's was produced. The resulting mass of ethanol adsorbed and desorbed in the film is shown in Fig. 6b. Notice that the change in mass does not occur instantaneously with the stepwise change in ethanol vapor concentration due to finite diffusion times of ethanol in the polymer. However, equilibrium is eventually achieved during the 470 second period of constant vapor concentration. The only exception is for the highest ethanol vapor concentration, 40 ppt, for which the mass signal is still increasing after 470 seconds. This may be due to the changing character of the Tecoflex as it becomes more like a concentrated polymer solution than a thin solid film. It is also clear from a comparison of Figs 6a and 6b that the change in adsorbed mass is approximately proportional to the change in ethanol vapor concentration, as indeed it should be if the polymer film is obeying Henry's law in its adsorption of ethanol. We have computed a partition coefficient or equilibrium constant for this process, as has been done by Grate and Abraham and coworkers for other polymer-gas systems [17, 18]. Details of these calculations will be presented elsewhere.

The thermal power dissipated in the Tecoflex film over the course of the same flow pattern is shown in Fig. 6c. The thermal signal is clearly not the time derivative of the mass signal in Fig. 6b. Indeed, there is little evidence of pulses of heat corresponding to the abrupt changes in mass. At the lowest ethanol vapor concentration the baseline thermal power of 14 μW is much higher than for the bare QCM, and the baseline itself shifts upwards as ethanol vapor concentration increases. Closer examination of peak shapes shows changes from cycle to cycle, particularly at ethanol vapor concentrations of 40 ppt.

The large offset in thermal baseline is due to an increase in thermal power generated by the QCM on the sample side. We believe that the change in peak shapes as ethanol vapor concentration increases from 20 to 40 ppt are due to the softening of the Tecoflex film and the corresponding increase in viscoelastic losses in the film. The Sauerbrey equation relating changes in mass per unit area with frequency shift, Eq. (1), is derived assuming that the thin layer is rigidly coupled to the underlying quartz crystal. For polymers, this assumption is questionable, as has been discussed by Bandey, Hillman, Brown, and Martin [19]. Exposure of polymers above their glass transition temperature to organic vapors can soften the films and change their viscoelastic properties. In effect, the complex shear modulus $G=G'+iG''$ of the polymer thin film is modified by gas adsorption and the resulting change in the shear storage modulus G' and the shear loss modulus G'' affects the acoustic coupling between the thin film and the quartz and the viscous dissipation of energy. In some circumstances this can lead to frequency shifts no longer simply related to mass changes by the Sauerbrey equation. If the complex impedance of the QCM is measured with an impedance analyzer, G' and G'' can in some cases be determined, as shown by Lucklum and Hauptmann [20].

Grate, Kaganove, and Bhethanabotla [21] have shown that thickness shear wave devices such as the QCM's employed here, when coated with rubbery polymers of ca. 1 μm thickness, behaved as gravimetric gas sensors (obeying the Sauerbrey equation) for low vapor concentrations. On the other hand, if the change in the shear loss modulus G'' is large enough, the effective resistance of the QCM at resonance, (R_1 in Fig. 4a) will increase, thus changing both the resonant current I and voltage V. The softened polymer film is damping the acoustical wave propagating in the film, and the damping energy is dissipated as heat. If this additional heat causes the increase in baseline and the unusual shapes of the peaks in Fig. 6c as we propose, such a contribution to the thermal power should be present in the QCM/HCC only when *rf* voltage is applied to the quartz resonator.

To test this hypothesis, the same flow pattern of ethanol vapor was repeated with the *rf* voltage to the sample QCM disconnected. Although no mass measurements can be taken in this mode, the good repeatability of the mass data evident in Fig. 6b assures that the thermal powers measured will correspond to the mass changes previously recorded under identical ethanol vapor concentrations. The resulting $P(t)$ signal is shown in Fig. 6d, where the different recording time periods have been aligned with the events of Figs 6a through 6c. Clear exothermic and endothermic heat pulses superimposed on a constant thermal baseline are observed, as expected. While there is some variation in amplitude of these pulses as the ethanol concentration changes, we show below that this variation is due to the non-zero thermal effects observed in Fig. 5. The integrated areas of the peaks in Fig. 6d are the heats evolved and absorbed in the film as it adsorbs and desorbs ethanol.

The data of Fig. 6 shows that with this apparatus we are able to subject a thin polymer film to a stepwise change in organic vapor concentration and directly to measure the corresponding mass changes Δm and heat changes Q for each sorption

Table 2 $\Delta_{sorption}H$ of ethanol in Tecoflex

Ethanol conc./ppt	Average Δm/μg	Tecoflex average heat/μJ	$\Delta_{sorption}H$/kJ mol^{-1}	Gold surface average heat/μJ	Corrected average heat/μJ	Corrected $\Delta_{sorption}H$/kJ mol^{-1}
45–40	–0.190	96	23	114	211	+51
40–35	–0.182	115	29	79	195	+49
35–30	–0.181	174	44	36	210	+53
30–20	–0.174	200	53	0	200	+53
25–20	–0.164	210	59	–8	201	+56
20–25	0.158	–214	–62	7	–207	–60
25–30	0.171	–200	–54	0	–200	–54
30–35	0.175	–169	–44	–29	–198	–52
35–40	0.153	–116	–35	–80	–196	–59
40–45	0.227	–89	–18	–113	–202	–41

event in the film. Because we measure both of these extensive quantities, we are in effect measuring the intensive quantity $\Delta_{sorption}H$, the molar enthalpy of sorption. The relationship is

$$\Delta_{sorption}H = [Q\ MM]/\Delta m \quad (5)$$

where *MM* is the molar mass of the organic vapor. To treat the data of Fig. 6, we averaged together the two or three mass changes Δm observed for a given step in ethanol vapor concentration, as well as averaging the several corresponding integrated heat pulses *Q*. These data are given in columns 1 through 3 of Table 2, and column 4 gives the resulting $\Delta_{sorption}H$ values. Note that if the concentration step sizes were infinitesimal, this quantity would be the thermodynamic *differential enthalpy of sorption*. $\Delta_{sorption}H$'s are positive in the first half of Table 2 because as ethanol vapor concentration is decreasing the resulting sorption enthalpies are endothermic, and *vice versa* for the last half of the table.

Under the assumption that the differential sorption enthalpy does not vary with ethanol vapor concentration, the $\Delta_{sorption}H$ values in column 4 should exhibit no systematic trend, but they do. The largest absolute values occur for the smallest ethanol concentrations. Figure 5, however, shows that for the highest ethanol concentrations there are significant background thermal signals even when no polymer film is present on the sample QCM. By integrating these background heat pulses of Fig. 5b we obtain the values of column 5 of Table 2, 'Gold surface Average Heat/μJ'. Notice that at the highest ethanol concentrations the background thermal effects exceed those due to absorption of ethanol by the Tecoflex film. However, the 'Tecoflex Average Heat' of column 3 may be corrected for the background signals of column 5, yielding the 'Corrected Average Heat' of column 6, and the resulting 'Corrected $\Delta_{sorption}H$' of column 7. There is now a much smaller and non-systematic variation in sorption enthalpy with changing ethanol concentration. Taking the mean and standard deviation of the five adsorption enthalpies and the five desorption enthalpies, we find that the molar enthalpy of adsorption of ethanol by Tecoflex SG-60 is –53±8 kJ mol^{-1}, and the molar enthalpy of desorption is +52±3 kJ mol^{-1}.

Discussion

There are no published values of the enthalpy of sorption of ethanol in Tecoflex. The value we obtain for desorption, 52 kJ mol^{-1}, is comparable to but somewhat larger than the enthalpy of vaporization of ethanol. The fact that the adsorption enthalpy is negative and the desorption enthalpy positive is in agreement with thermodynamic expectations. While the background corrections to the thermal signals are not small compared to some of the signals themselves, the easiest way to minimize background contributions is to increase the surface area of the film. The available area on the QCM surface is 1.3 cm^2, but the sample area was only 0.16 cm^2. Drop-coating is not the best method of making uniform thin films. We are now using spin-coating.

We have demonstrated that sorption enthalpies in a thin polymer film can be determined by measuring with high precision both the mass change and the heat flow when that film is exposed to ethanol vapor. We have also made similar measurements of the sorption by Tecoflex of other organic vapors, and will present these results elsewhere. Any polymer above its glass transition temperature should absorb and desorb gases such as water vapor and organic solvents, and determining sorption enthalpies is a way of characterizing such polymer-solvent systems in the region of high polymer weight fraction. Many measurements of solubility of organic vapors in polymers using inverse gas chromatography have reported sorption enthalpies derived from van't Hoff analysis of the change in partition coefficients with temperature. A typical example is recent work by Gavara, Hernandez and coworkers on the solubility of alcohols in ethylene-vinyl alcohol copolymers [22]. It is surprising that these workers find an endothermic enthalpy of adsorption ('solution') above the glass transition temperature, at variance with our findings.

Quartz microbalance microcalorimetry is superior to inverse gas chromatography in several respects. In the latter, a retention time (or volume) is measured and related to a gas-polymer partition coefficient under the *assumption* of equilibration between mobile and stationary phase. In our apparatus we directly *observe* the establishment of equilibrium, by changing the gas composition and waiting until the resulting mass change and heat flow signals have reached steady-state. In inverse gas chromatography, sorption enthalpies are derived under the assumption that the polymer phase does not change its properties with temperature above T_g, but this is not the case. In quartz microbalance microcalorimetry, the determination of sorption enthalpies are made isothermally and directly by measuring mass and heat.

Although we do not report the ethanol-Tecoflex partition coefficient or equilibrium constant K_{sorption}, it is clear that the data of Fig. 6 are sufficient to determine this quantity. From K_{sorption} the Gibbs energy of sorption can be determined, and the resulting sorption entropy is calculable as $(\Delta_{\text{sorption}}H - \Delta_{\text{sorption}}G)/T$. A single set of isothermal measurements is thus sufficient to determine the three basic thermodynamic quantities which characterize polymer-solvent systems in one region of their phase diagram.

Quartz microbalance microcalorimetry need not be limited to organic gases interacting with polymer films. Studying the hydration and dehydration of thin protein films and other films of biological interest with this technique should permit direct measurement of the thermodynamic quantities which characterize the interaction of water with biological molecules. The film could be inorganic or metallic: in our laboratory we have observed mass change and heat flow signals when hydrogen gas is adsorbed by a thin palladium film plated on the QCM [23]. The gas need not just be adsorbed by the film; it could react with the film to form solid or volatile products. If the surface is a catalyst, one could study the thermodynamics of the poisoning of the catalyst. On a more practical note, chemical vapor sensors based on gravimetric detectors such as surface acoustic wave sensors or QCM's [7, 24] are well developed but these sensors are not very selective because they measure only one extensive variable, mass update by the coating deposited on the sensor. The mass/heat flow sensor discussed here can in principle

measure simultaneously two extensive quantities, mass uptake and heat flow, and the ratio of these quantities is an intensive quantity (enthalpy of sorption) characteristic of the gaseous molecule and the adsorbing surface. Thus, gas sensors based on the QCM/HCC concept should be much more selective than QCM sensors and just as sensitive.

Conclusions

We have developed a new, highly sensitive experimental approach to determining enthalpy changes for gas-surface interactions: quartz microbalance microcalorimetry. Employing only 12.7 μg of Tecoflex, an aliphatic polyurethane, we measured the molar enthalpy of adsorption of ethanol in a thin Tecoflex film to be –53±8 kJ mol^{-1}, and the molar enthalpy of desorption to be +52±3 kJ mol^{-1}.

Note

We feel obliged to inform readers of experiments conducted after the review of this paper. We now have more efficient mixing of the gases and therefore identical vapor compositions in both reference and sample cells. We also use spin-coating instead of drop-coating for thin film preparations, which allows us to deposit thinner and more uniform films over the entire QCM surface. Finally, a new technology (the active-bridge oscillator) kindly provided to us by Mr. Kurt Wessendorf of Sandia National Laboratories can monitor slight changes in the resistance of the coated QCM due to changes in the viscoelastic properties of the coating material. As we repeated the Tecoflex sorption experiment with ethanol and other organic vapors under these conditions, we immediately observed the results of the improvements. Detailed description of this new set of experiments will be presented elsewhere, but a few important points relevant to this paper are as follows:

1. Corrections in the thermal traces are no longer necessary, since the sample and the reference have identical vapor compositions.

2. With the new, thinner, spin-coated Tecoflex film on the QCM there was virtually no change in the QCM's resistance during sorption/desorption cycles. This was apparent both in the thermal traces (no shift in the base-line) and also in direct resistance measurements using the active-bridge oscillator. Therefore even when the QCM is in operation, the heat measured is entirely due to sorption.

3. The measured $\Delta_{sorption}H$ for ethanol in Tecoflex was 44 kJ mol^{-1}, a value much closer to the $\Delta_{vaporization}H$ of ethanol itself (42.3 kJ mol^{-1}). Similar results were also obtained for other organic vapors with the exception of chlorinated compounds such as chloroform.

* * *

ALS would like to thank Professor Ingemar Wadsö of Lund University, in whose laboratory we originated the QCM/HCC concept. The QCM/HCC was built at Lund with the design and construction assistance of Professor Wadsö. We thank Professor Richard Beard for the loan of the impedance analyzer.

References

1 F. Gundert and B. A. Wolf, in J. Brandrup, I. E. H. (Eds.): Polymer Handbook, John Wiley & Sons, New York 1989, p. VII/173–VII/182.
2 E. A. Grulke, in J. Brandrup and E. H. Immergut (Eds.): Polymer Handbook, John Wiley & Sons, New York 1989, p. VII/519–VII/560.
3 R. A. Orwoll, in J. Brandrup and E. H. Immergut (Eds.): Polymer Handbook, John Wiley & Sons, New York 1989, p. VII/497–VII/516.
4 D. R. Lloyd, T. C. Ward and H. P. Schreiber, Inverse Gas Chromatography: Characterization of Polymers and Other Materials, Vol. 391, American Chemical Society, Washington DC 1989.
5 A. L. Smith, H. Shirazi and I. Wadsö, Recent Advances in the Chemistry and Physics of Fullerenes and Related Materials (San Diego, CA), The OCM/HCC: simultaneous, isothermal, high sensitivity measurements of mass change and heat flow in polymer and fullerene films, pp. 576–585 (1998).
6 M. D. Ward and D. A. Buttry, Science, 249 (1990) 1000.
7 J. W. Grate, S. J. Martin and R. M. White, Analytical Chemistry, 65 (1993) 940A–948A, 987A–996A.
8 G. Sauerbrey, Z. Physik, 155 (1959) 206.
9 J. F. Alder and J. J. McCallum, Analyst, 108 (1983) 1169.
10 J. J. McCallum, Analyst, 114 (1989) 1173.
11 I. Wadsö, Chem. Soc. Rev., 1997 (1997) 79.
12 S. J. Martin, V. E. Granstaff and G. C. Frye, Anal. Chem., 63 (1991) 2272.
13 J. Auge, P. Hauptmann, J. Hartmann, S. Rosler and R. Lucklum, Sensors and Actuators B, 24–25 (1995) 43.
14 V. Tsionsky and E. Gileadi, Langmuir, 10 (1994) 2830.
15 D. A. Buttry and M. D. Ward, Chemical Reviews, 92 (1992) 1355.
16 R. Zhou, A. Hierlemann, U. Weimar and W. Göpel, Sensors and Actuators B, 34 (1996) 356.
17 J. W. Grate, A. Snow, D. S. Ballantine, H. Wohltjen, M. H. Abraham, R. A. McGill and P. Sasson, Anal. Chem., 60 (1988) 869.
18 J. W. Grate, S. N. Kaganova and V. R. Bhethanabotla, Anal. Chem., 70 (1998) 199.
19 H. L. Bandey, A. R. Hillman, M. J. Brown and S. J. Martin, Faraday Discussion, 107 (1997) 105.
20 R. Lucklum and P. Hauptmann, Faraday Discussion, 107 (1997) 123.
21 J. W. Grate, S. N. Kaganove and V. R. Bhethanabotla, Faraday Discussion, 107 (1997) 259.
22 R. Gavara, R. Catala, S. Aucejo, D. Cabedo and R. Hernandez, J. Poly. Sci. B: Polymer Phys., 34 (1996) 1907.
23 H. Shirazi, A. L. Smith and D. Schneider, in preparation.
24 J. W. Grate, M. H. Abraham and R. A. McGill, in E. Kress–Rogers (Ed.): Handbook of Biosensors and Electronic Noises, CRC Press, Boca Raton 1997, p. 593–612.